Trauma Monthly 2023; 28(6): 994- 1002

10.30491/tm.2023.418522.1648

Trauma Monthly

Research Article

Electrospun Fibrous Membrane Containing Pistachio Hull Extract /Polyvinyl Alcohol as Accelerator Healing of Calvarial Defects in Wistar Rats

Mahshid Farmand [1], Hamid Reza Moslemi [1*], Mohammad Hassan Yousefi [2], Sahar Ghaffari Khaligh [3]

[1] Department of Clinical Sciences, Faculty of Veterinary Medicine, Semnan University, Semnan, Iran.
[2] Department of basic Sciences, Faculty of Veterinary Medicine, Semnan University, Semnan, Iran.
[3] Department of Pathobiology, Faculty of Veterinary Medicine, Semnan University, Semnan, Iran.

***Corresponding Author**: Hamid Reza Moslemi; Department of Clinical Sciences, Faculty of Veterinary Medicine, Semnan University, Semnan, Iran, Tel: 0098-23-31532607 & Fax: 0098-23-31532626, Email: h.moslemi@Semnan.ac.ir

Received 2023-09-29; **Accepted** 2023-12-25; **Online Published** 2023-12-29

Abstract

Introduction: Fracture healing is a major concern in orthopedic surgery, necessitating the identification of new techniques with minimal side effects to expedite the healing process. This study aimed to evaluate the effect of topical nanofibers loaded with Pistachio hull extract on the healing of bone defects in rat calvaria

Methods: Defects of 7 mm were induced in the calvaria of 45 male Wistar rats. The animals were divided into three groups, with defects in each group being treated with nanofibers loaded with Pistachio hull extract (PVA-PH), PVA nanofibers (PVA), or left empty as a control group. Histopathological evaluation was conducted on days 14, 28, and 42.

Results: On day 14, a significant difference was observed between the PVA/PH and the control, while no significant difference was found between the PVA/PH and PVA. As the days progressed to 28 and 42, the PVA/PH exhibited a significantly higher healing rate compared to both the PVA and controls.

Conclusions: The results from this study demonstrate that nanofibers loaded with pistachio hull extract can significantly enhance osteogenesis and promote the healing process of calvarial defects in rats over a 42-day period. This finding holds promise for developing improved approaches to facilitate fracture healing with reduced side effects.

Keywords: Electrospinning, Pistachio hull extract, Calvarium.

Introduction

Effective bone regeneration depends on several key factors, including precise analysis, specific materials, appropriate growth factors, and molecules working together. Oxidative stress has a significant impact on bone regeneration by disrupting the balance between osteoblasts and osteoclasts, potentially leading to bone-related disorders. To manage oxidative stress, it's crucial to administer antioxidant agents that can mitigate the harmful effects of reactive oxygen species (ROS). Custom-designed scaffolds with low cytotoxicity and excellent biocompatibility can also enhance bone regeneration by providing a solid foundation for tissue restoration and remodeling.[1] In recent decades, there has been a growing focus among researchers on expediting the healing process of bone fractures. Accelerated bone healing has been employed in the treatment of fractures, non-union fractures, osteomyelitis, bone lengthening procedures, bone tumor resection, joint fusion, and joint prostheses. Since the natural healing of bones is a time-consuming process and non-healing fractures can occur, the exploration of alternative therapies is desirable and imperative. Nowadays, several methods for bone regeneration are being employed, including the

utilization of various materials as bone substitutes and accelerators for bone healing.[2,3]

Biomaterials and scaffolds play a crucial role in promoting healthy tissue formation, particularly in fields like bone regeneration. The key to success lies in using materials that mimic the extracellular matrix (ECM) and are bioactive. Achieving proper healing involves a combination of nanotechnology and herbal medicine applications. Nanoscale materials offer a larger surface area for drug release and matrix degradation, enhancing the healing process. Among various nanotechnological methods, electrospinning is the most commonly used technique for producing uniform fibers from different materials.[4-8]

Medicinal plants have a rich history in treating diseases due to their empirically discovered health benefits. However, their use has declined over time due to factors like population growth, urbanization, and scientific advancements. Chemical substances and drugs have largely replaced medicinal plants in many cases.[8]

Pistachio (Pistacia vera L.), native to arid regions in Central and West Asia and found across the Mediterranean basin, is renowned as one of the most popular tree nuts. Over the past two decades, global pistachio production has experienced a significant rise, reaching an estimated 10,057,566 tons. The leading producers include the United States of America (36%), Iran (32%), Turkey (16%), China (7.5%), and Syria (5%).

The industrial processing of pistachios generates a significant amount of waste, with hulls accounting for 35 to 45% of the discarded material. Improper disposal of these hulls can lead to environmental pollution. However, recent research has revealed that pistachio hulls contain valuable phenolic compounds similar to those in known sources of phenolics. By utilizing these hulls as a source of phytochemicals, not only adds value to pistachio production but also offers a practical solution for managing this abundant by-product and reducing environmental impact.[9-11]

Accordingly, the present study aimed to evaluate the effect of polyvinyl alcohol (PVA) nanofibers containing pistachio hull extract on the treatment of calvarial defects in rats.

Methods

Pistachio Hull Extract Preparation

The pistachio hulls (PH) were obtained from the Damghan Agricultural Research Center in Iran and their species were verified and documented at the herbarium of the Semnan Agriculture and Natural Resources Research Center. The hulls were thoroughly washed and dried under dark conditions without the application of heat, after which they were powdered using an electric grinder. A total of 30 g of the prepared powder was placed in a filter paper thimble and inserted into the extraction chamber of a Soxhlet apparatus. Extraction was carried out using 250 mL of ethanol (80% v/v) at a temperature of 70°C for 4 hours. The resulting solution was then transferred to a rotary evaporator to remove the solvent and concentrate the extract. To separate the liquid extract from the solid residue, vacuum filtration was performed using sterile cellulose nitrate membrane filters (0.45 μm). Finally, the liquid extracts were stored in sterile glass containers at a temperature of 4°C to maintain their integrity and purity.[12,13]

Antioxidant activity

The hydrogen atom or electron donation capabilities of the corresponding extracts and specific pure compounds were determined by observing the decolorization of a purple methanol solution containing 2,2-diphenyl-1-picrylhydrazyl (DPPH). This spectrophotometric assay utilized the stable radical DPPH as a reagent, following the method established by Burits and Bucar.[14] In summary, 50 μL of the extract was mixed with 5 mL of a DPPH solution (0.004% methanol solution). After a 30-minute incubation at room temperature, the absorbance was measured against pure methanol at 517 nm. The sample's radical-scavenging activities were quantified as inhibition percentages using the following equation: $I\% = (A_{blank} - A_{sample/Ablank}) \times 100$; where A_{blank} represents the absorbance of the control (containing all reagents except the test compound), and A_{sample} is the absorbance of the test compound. The concentration of the extract required to achieve 50% inhibition (IC50) was calculated from the plot of inhibition percentages against extract concentration using PHARM/PCS-version 4.

Fabrication of pistachio hull-loaded Nanofibers

A solution of PVA (polyvinyl alcohol) with a molecular weight of approximately 72,000 from Merk, Germany, was prepared by dissolving it in distilled water at a

concentration of 10% w/v. The solution was stirred for 3 hours at 80°C to achieve a homogeneous mixture. Simultaneously, a solution of pistachio hulls was prepared in distilled water at a concentration of 100 mg/ml. Different ratios of the PVA and pistachio hull solutions were blended, namely 100:0, 90:10 and 80:20 (v/v%). The electrospinning process was conducted under specific conditions, including an applied voltage of 15 kV, a distance of 18 cm between the needle tip and collector, and a feed rate of 2.5 ml/h, with the collector rotating at a speed of 300 rpm. The resulting films incorporated pistachio hulls at final concentrations of 10 and 20 mg/ml, respectively.

Characterizations of Electrospun pistachio hull-loaded Nanofibers

Scanning electron microscopy (SEM, XL30 Philips) was used to examine the surface morphologies and microstructures of both PVA and PVA/PH nanofibers. To facilitate the analysis, a thin layer of gold was applied to coat the nanofibers. The average diameter of the nanofibers was determined using Image J software.

In order to identify the chemical structures of the extract and nanofibers, a Fourier Transforms Infrared spectrometer (FTIR, Shimadzu FTIR 8400S spectrophotometer) was employed. The spectra were collected at room temperature within the wavelength range of 400-4000 cm-1.

Animals

45 male Wistar rats, about 300 g and 4 months old, were used. To reduce stress and help the rats adjust to their environment, they were kept in consistent environmental and nutritional conditions for a duration of one week. These conditions included maintaining a stable temperature, humidity, lighting, food type, and meal frequency. The rats were provided with specialized laboratory animal feed pellets and had unrestricted access to water.

Surgical procedure

The dorsal part of the cranium was shaved and disinfected. A 5 cm midline incision, over the external sagittal crest, was made. After the calvarium was exposed, a 7 mm circular bone defect was created with a trephine bur. The depth of the cavity reached the meningeal membrane, allowing the drill bit to detect its softness. The cavities were filled with dressing composed of nanofibers loaded with pistachio hull extract (PVA-PH group) in the first group and PVA dressing (PVA group) in the second group. The third group, designated as the control group, remained untreated and empty. The incisions were closed using a simple interrupted pattern with 3-0 nylon sutures. Postoperatively, all animals received cefazolin (30 mg/kg, twice a day for 3 days) and flunixin meglumine (20 mg/kg, once a day for 3 days).

Specimen preparation and histological evaluation

Animals were euthanized on 14, 28, and 42 days using an over dose of thiopental. The skin surrounding the original surgical defect on the animals' calvarium bone was carefully dissected and removed en bloc with the adjacent tissues. The excised tissue was immediately placed in 10% neutral buffered formalin. Subsequently, it was rinsed with water and demineralized using 10% formic acid. After decalcification, each specimen was longitudinally divided into two blocks in the sagittal direction and embedded in paraffin. Longitudinal serial sections were then cut, starting from the center of the surgical defect. These sections were stained with hematoxylin and eosin, as well as Masson's Trichrome, for further analysis.

Blinded to the treatments, two investigators assessed the images and assigned scores ranging from 1 to 10 based on several parameters. These parameters included the amount of new bone formation, the quality of the bone (woven or lamellar), the degree of vascularization, and the presence or absence of inflammation, following Musson's grading system.[15]

Data Analysis

The statistical analysis utilized SPSS software version 16.0 (SPSS Inc., USA) along with the Kruskal-Wallis test. The data were presented as the mean ± standard deviation (SD). Significance was determined by a p-value less than 0.05.

Results

Morphology of the PVA and PVA/PH

Figure 1 illustrates the morphology of pure PVA and PVA/PH nanofiber scaffolds at various ratios. The findings indicate that the pure PVA and PVA/PH scaffolds with a ratio of 90:10 (v/v) exhibit smooth and thin nanofibers without any bead formation. This suggests that the PSE extracts are effectively incorporated within the nanofibers, resulting in a uniform structure. However, in the 80:20 (v/v) ratio, the

uniformity and smoothness of the fibers are reduced. This could be attributed to the higher viscosity and concentration of the solution, which impacts the morphology of the nanofibers. Based on these observations, the PVA/PH ratio of 90:10 (v/v) was selected for further analysis.

The average diameter of the pure PVA and PVA/PH nanofiber scaffolds at the 90:10 (v/v) ratio was measured as 482±61 nm and 549±189 nm, respectively. These results indicate that an increase in the concentration of PH leads to an enlargement in the diameter of the fibers.

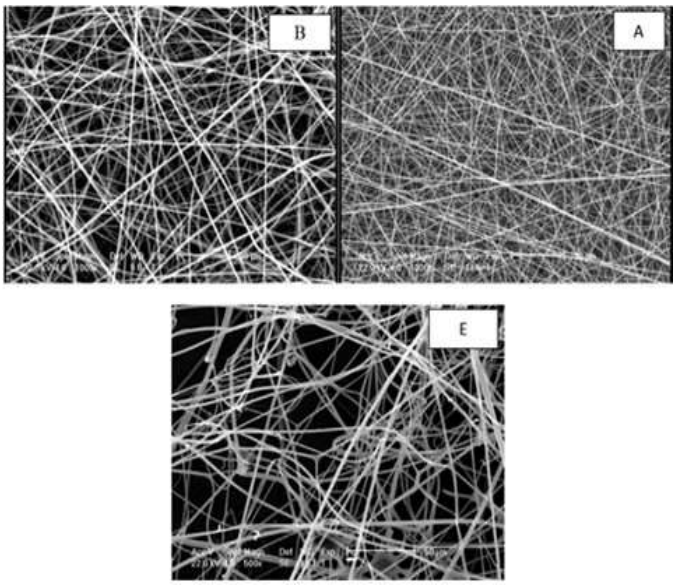

Figure 1: SEM images of (A) PVA, (B) PVA/PH (90:10 (v/v)), (E) PVA/PH nanofibers (80:20 (v/v)). The final concentration of the PH incorporated into each film was 10 and 20 mg/ml respectively.

FT-IR Analysis

FT-IR spectra were employed to validate the distinctive peaks of both pure PVA and PVA/PH nanofibrous scaffolds (Figure 2). The peak at 848 cm-1 corresponds to the rocking vibration of C-H bonds within the PVA structure. Absorption peaks at around 1093 cm-1 and 1255 cm-1 are linked to the stretching vibration of C-O and C-OH bonds in the PVA structure. Moreover, a visible absorption band observed at approximately 1382 cm-1 and 1413 cm-1 indicates the bending vibrations of C-H bonds in the chemical composition. The absorption peak near 1730 cm-1 is attributed to vibrations of the C=O bond from residual acetate within the PVA originating from the raw materials used, specifically polyvinyl acetate. Weak absorption peaks ranging from 2820 cm-1 to 2924 cm-1 are associated with the symmetric and asymmetric stretching vibrations of aliphatic C-H bonds in the polyvinyl alcohol structure. Additionally, the broad absorption peak at 3346 cm-1 corresponds to vibrations of O-H bonds found in the hydroxyl groups of the PVA structure.

Peaks of PVA/PH nanofibrous scaffold include the stretching vibration of O-H bonds within the range of 3000 cm-1 to 3800 cm-1, which can result from the presence of hydroxyl groups within the compound structure or absorption of environmental moisture on the material's surface. Furthermore, peaks associated with the asymmetric and symmetric stretching vibrations of C-H bonds in alkyl groups, stretching vibrations of C=O bonds, stretching vibrations of C=C bonds within aromatic rings, bending vibrations of C-H bonds, stretching vibrations of C-O bonds in C-O-C and C-OH functional groups, and bending vibrations of C-H bonds attached to aromatic rings in the extract structure are evident. These peaks confirm the presence of cellulose and lignin compounds as the primary constituents within the pistachio hull extract incorporated in the fibers. Notably, the samples containing pistachio hull extract display a new peak at approximately 1590 cm-1, corresponding to the stretching vibration of C=C bonds within the aromatic rings of the extract. This peak serves as further evidence of the extract compounds' presence within the composite structure.

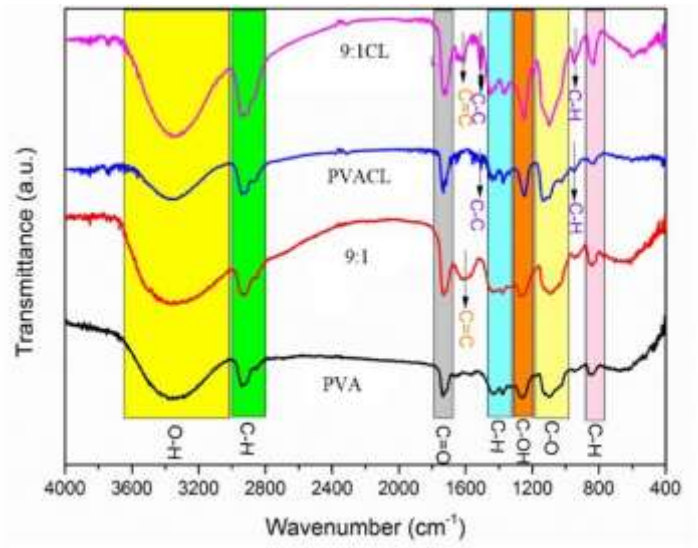

Figure 2: Fourier transforms infrared spectra of PVA and PVA/PH nanofibers (90:10 (v/v)).

Free radical-scavenging activity

The in vitro antioxidant activities of Pistachio hull extract and beta-hydroxy toluene (BHT) in the DPPH assay were found to be 0.02 µg/ml and 4.9 µg/ml, respectively. Notably, the extract exhibited higher free radical-scavenging activities compared to BHT. Moreover, the results demonstrated that an increase in extract concentration led to a corresponding increase in free radical-scavenging activity. High IC50 values indicated low antioxidant activity.

Histopathological Examination

Table 1 presents the results of histopathological studies. On day 14, significant differences were observed between the groups of PVA/PH and PVA nanofibers when compared to the control group ($p \leq 0.05$). However, no significant difference was found between the PVA/PH and PVA groups ($p > 0.05$). In the control group, there was very little bone defect coverage, along with a lack of new bone formation, low angiogenesis, and relatively high inflammation. In contrast, the PVA group showed moderate angiogenesis, and in the group treated with nanofibers containing extract, both angiogenesis and moderate inflammation were observed (Fig. 3).

On day 28, there was a significant difference between the PVA-PH group and control and PVA groups ($p \leq 0.05$); however, there was no significant difference between the control and the PVA groups ($p > 0.05$). In the control group, there was very low coverage of the bone defect, along with the creation of immature bone tissue (Woven), noticeable angiogenesis, and moderate inflammation. The PVA group showed no new bone formation but had high levels of angiogenesis. In the PVA/PH group, there was also low coverage of the bone defect, the creation of immature bone tissue (Woven), significant angiogenesis, and moderate inflammation (Fig. 4).

The results revealed a significant difference between the PVA-PH group and the control as well as PVA groups on day 42 ($p \leq 0.05$). Also, there was no significant difference between PVA and control groups ($p > 0.05$). In the control group, there was very low bone defect coverage, a lack of new bone formation along with angiogenesis, and moderate inflammation. In the PVA group, medium-sized fibroblasts with thin and curly collagen fibers were observed, along with low angiogenesis. In contrast, the PVA/PH group showed distinct differences from the previous two groups. It exhibited complete coverage of the bone defect, the formation of immature bone tissue (Woven), noticeable angiogenesis, and low levels of inflammation (Fig. 5).

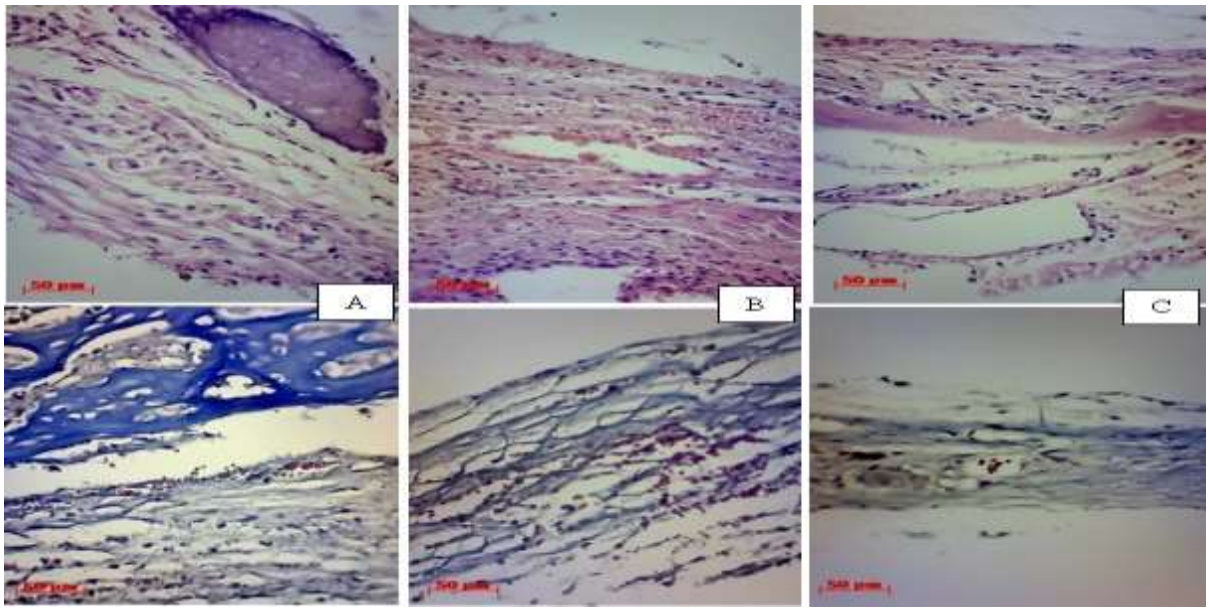

Figure 3: Photomicrograph of all groups on day 14 post-operation; (A) PVA-PH group: Relatively thick collagen fibers were observed, along with a relatively low number of fibroblasts and angiogenesis.; (B) PVA Group: A relatively high number of fibroblasts were present, along with very thin collagen fibers and low levels of angiogenesis.; (C) Control Group: A high number of fibroblasts were observed, along with very thin collagen fibers and a significant level of angiogenesis. (Top row: H&E and Bottom row: Masson's Trichrome, ×100).

Table 1: The Mean ± SD of the histopathological changes in all groups.

	14	28	42
Control	1.67 ± 0.57 [a]	3 ± 1.22 [a]	3.5 ± 0.57 [a]
PVA	2.67 ± 0.57 [b]	3 ± 0.81 [a]	3.4 ± 0.54 [a]
PVA-PH	3.33 ± 0.57 [b]	5 [b]	6.4 ± 0.89 [b]
There was no significant difference between the same letters in each column, but a significant difference was observed between the non-identical letters. The difference was significant ($p \leq 0.05$).			

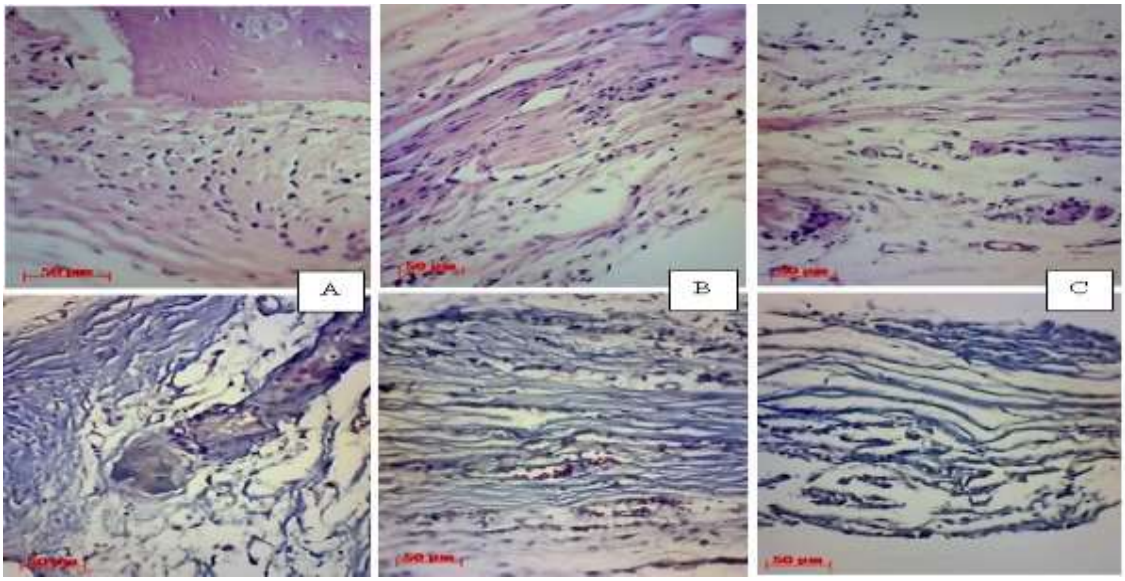

Figure 4: Photomicrograph of all groups on day 28 post-operation; (A) PVA-PH group: thick collagen fibers and a low number of fibroblasts, as well as low levels of angiogenesis were observed; (B) PVA Group: Moderate fibroblast presence with very thin and curly collagen fibers, along with relatively low levels of angiogenesis, were observed; (C) Control Group: A significant number of fibroblasts with thin collagen fibers and abundant angiogenesis were observed. (Top row: H&E and Bottom row: Masson's Trichrome, ×100).

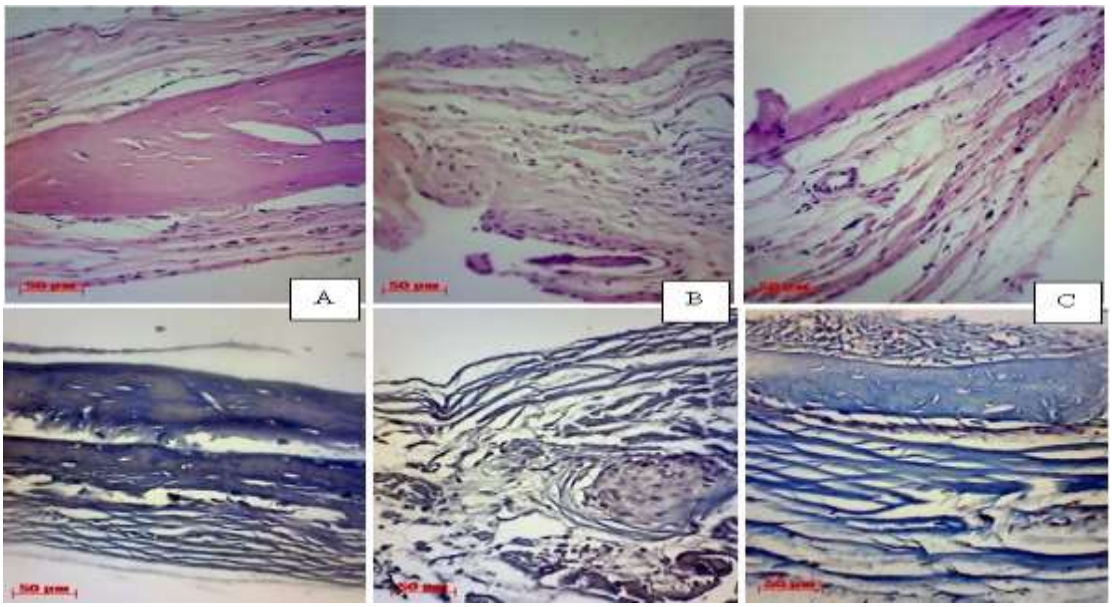

Figure 5: Photomicrograph of all groups on day 42 post-operation; (A) PVA-PH group: full coverage of the bone defect, the creation of immature bone tissue (Woven), thick and parallel collagen fibers, a significant number of fibroblasts, and very little angiogenesis were observed; (B) PVA Group: Medium-sized fibroblasts with thin and curly collagen fibers were present, and angiogenesis was low were observed; (C) Control Group: Thin collagen fibers and fibroblasts were observed, along with high levels of angiogenesis were observed. (Top row: H&E and Bottom row: Masson's Trichrome, ×100).

Discussion

The increasing economic burden of fracture healing is becoming particularly concerning for healthcare systems in developing nations. This study focused on the successful development of a PVA/PH nanofibrous scaffold with desirable properties for fracture healing in rat calvaria. The scaffold was enriched with phenolic compounds sourced from pistachio hulls, which have known for their strong antioxidant and antibacterial properties. To achieve these properties, electrospinning was conducted to produce uniform nanofibrous PVA/PH in various ratios. The optimal combination was determined to be 0.9:10 mg/ml of PVA/PH. This fabricated nanofibrous mat exhibited a uniform structure, devoid of beads, indicated the scaffold's mechanical integrity and potential suitability for fracture management. Notably, the optimized PVA/PH ratio played a pivotal role in achieving this uniformity and enhancing the scaffold's overall effectiveness. Previous studies supported these findings, demonstrating that the concentration of extracts in PVA scaffolds strongly influenced the nanofiber characteristics, with higher extract concentrations leading to increased fiber diameters and the presence of beads.[16,17] However, despite the addition of PH, the main intensive peak characteristic of the semi-crystalline structure and intermolecular hydrogen bonding in PVA scaffolds remained unchanged.

The results of our study on day 14 revealed that a significant difference between the PVA/PH group and the control group, while no significant difference was found between the PVA/PH and PVA groups. As time progressed to days 28 and 42, the PVA/PH group exhibited a significantly higher healing rate compared to both the PVA and control groups. Notably, the PVA/PH group showed a consistently superior healing response throughout the study, suggesting the beneficial impact of nanofibers loaded with pistachio hull extract on the osteogenesis process.

Oxidative stress significantly impacts the process of bone regeneration, leading to delayed bone healing. The imbalance between osteoblasts and osteoclasts can expose the bone to prolonged oxidative stress, resulting in cellular senescence, skeletal disorders, and bone diseases. Therefore, managing oxidative stress levels during bone healing becomes crucial. To mitigate the harmful effects of reactive oxygen species (ROS), administering antioxidant agents holds promise in reducing oxidative stress. Research has shown that natural antioxidants have the potential to restore bone parameters and facilitate the formation, regeneration, and mineralization of bone tissue.[1] As a result, the use of natural antioxidants to enhance bone healing has become a central focus in current research. This finding aligns with a previous study that highlighted the osteo-protective effects of green tea. In this study, green tea demonstrated its ability to decrease oxidative stress, increase the activity of antioxidant enzymes, and reduce the expression of proinflammatory mediators in various rodent bone loss models.[18,19] Furthermore, our current study suggests that the extract derived from pistachio hull has the potential to effectively prevent the development of oxidative stress-induced damage in bone tissue. Numerous studies have attested to the remarkable antioxidant capacity of pistachio hull extract.[13,20] The compounds present in pistachio hull seem to prevent the formation of free radicals and can accelerate the healing process of bone defects due to their antioxidant and anti-inflammatory activities. Previous research has highlighted the antioxidant properties of phenolic and flavonoid compounds present in herbs, indicating their potential in combating oxidative stress.[21] Particularly, among antioxidants, phenolic compounds have demonstrated robust reducing properties. The positive effects of phenolic compounds primarily arise from their antioxidant characteristics, as they act as scavengers of reactive oxygen species (ROS). These properties stem from their potential to reduce and their unique chemical structure, enabling them to counteract free radicals, form complexes with metal ions, and quench molecules of triplet oxygen.[22]

In our investigation, we discovered that pistachio hulls are rich in phenolic compounds. Given these properties, phenols could influence bone metabolism by suppressing inflammatory mediators[23], including cytokines that play a significant role in supporting osteoclast differentiation and resorption. Consequently, this leads to a reduction in bone resorption.[24] Furthermore, phenols have demonstrated the ability to activate the Mitogen-Activated Protein Kinases (MAPKs) signaling pathway in various cellular systems, employing both direct and indirect mechanisms. Targeting the MAPKs pathway allows these compounds

to exert positive effects on bone metabolism. As a result, they regulate osteoclast differentiation, bone resorption, and facilitate osteoblast proliferation, differentiation, and functional activities. Additionally, phenols have been observed to negatively modulate genes associated with receptor activator κB ligand (RANKL)-induced osteoclast differentiation, such as NFATc1 [25], c-fos [26], NF-jB, and AP-1.[27,28] This regulatory process involves the modulation of extracellular signal-regulated kinases (ERK1/2), p38, and c-Jun- N terminal kinase (JNK) MAPKs expression and phosphorylation.[29-31]

Phenolic compounds play a significant role in preserving bone health, operating through five potential mechanisms: (i) Reducing bone loss by leveraging antioxidant activity, (ii) Diminishing bone loss via anti-inflammatory action, (iii) Enhancing osteoblastogenesis, (iv) Reducing osteoclastogenesis, and (v) Engaging in osteoimmunological activity.[32]

On the other hand, when bacterial or fungal infections are present at the site of injury, particularly in open fractures, they can cause a delay in bone healing. In such cases, the incorporation of pistachio hull, which possesses favorable antimicrobial properties [12,33], has been confirmed in various studies, making it a suitable candidate for fabricating this nanofibrous mat.

The phenolic compounds present in pistachio hull possess potent antibacterial properties attributed to their unique molecular structure. These compounds exert their effects at the cellular level through various mechanisms. Such activities are believed to involve alterations in cell membrane permeability, intracellular functions influenced by hydrogen bonding of phenolic compounds to enzymes, and changes in cell wall stiffness leading to the loss of integrity through interactions with cell membrane. [35]

Conclusion

The findings from this study indicate that nanofibers loaded with pistachio hull extract can significantly enhance osteogenesis and promote the healing process of calvarial defect in rat calvarium over a 42-day period. Therefore, the use of these nanofibers in orthopedic surgical procedures appears promising candidate for promoting fracture healing and advancing regenerative medicine approaches, given their potential role in facilitating bone healing.

Acknowledgments

The authors would like to thank the patients and personnel of Golestan Hospital for their cooperation in performing the present study.

Conflict of Interest Disclosures

The authors declare that they have no Conflict of Interest.

Funding Sources

None.

Authors' Contributions

All the authors contributed in designing, collecting, analyzing editing the final manuscript.

Ethical Statement

The research protocol received ethical approval from the Ethical Committee for Research at Semnan University's Faculty of Veterinary Medicine in Iran (Approval number: IR.SU.REC.1400.15).

References

1. Badila AE, Radulescu DM, Ilie A, Niculescu A, Grumezescu AM, Radulescu AR. Bone Regeneration and Oxidative Stress: An Updated Overview. Antioxidants. 2022; 11: 1-22.

2. Silber JS, Anderson DG, Daffner SD, Brislin BT, Leland JM, Hilibrand AS, et al. Donor site morbidity after anterior iliac crest bone harvest for single-level anterior cervical discectomy and fusion. Spine. 2003; 28: 134-9.

3. Ebraheim NA, Elgafy H. Bone-graft harvesting from iliac and fibular donor sites: techniques and complications. J. Am. Acad. Orthop. Sur. 2001; 9: 210-8.

4. Sriyanti ID, Edikresnha D, Rahma A, Munir MM, Rachmawati H, Khairurrijal K. Mangosteen pericarp extract embedded in electrospun PVP nanofiber mats: physicochemical properties and release mechanism of α-mangostin. Int. J. Nanomedicine. 2018; 13: 4927-41.

5. Edikresnha D, Suciati T, Munir MM, Khairurrijal K. Polyvinylpyrrolidone/cellulose acetate electrospun composite nanofibres loaded by glycerine and garlic extract with in vitro antibacterial activity and release behaviour test. RSC Adv. 2019; 9: 26351-63.

6. Xue J, Wu T, Dai Y, Xia Y. Electrospinning and Electrospun Nanofibers: Methods, Materials, and Applications. Chem. Rev. 2019; 119: 5298-415.

7. Niemczyk-Soczynska B, Gradys A, Sajkiewicz P. Hydrophilic Surface Functionalization of Electrospun Nanofibrous Scaffolds in Tissue Engineering. Polym. 2020; 12: 2636-56.

8. Firenzuoli F, Gori L. Herbal Medicine Today: Clinical and Research Issues. Evid. Based. Complement. Alternat. Med. 2007; 4: 37-40.

9. Ennouri K, Ayed RB, Hlima HB, Smaoui S, Gouiaa M, Triki MA. Analysis of variability in Pistacia vera L. fruit genotypes based on morphological attributes and biometric techniques. Acta Physiol. Plant. 2020; 42.

10. Arjeh E, Akhavan HR, Barzegar M, Carbonell-Barrachina AA. Bio-active compounds and functional properties of pistachio hull: a review. Trends Food Sci. Technol. 2020; 97: 55–64.

11. Elhadef K, Akermi S, Ben Hlima H, Ennouri K, Fourati M, Ben Braiek O, et al. Tunisian Pistachio Hull Extracts: Phytochemical Content, Antioxidant Activity, and Foodborne Pathogen Inhibition. J. Food Qual. 2021; 2021: 1-18.

12. Rajaei A, Barzegar M, Mobarez AM, Sahari MA, Esfahani ZH. Antioxidant, anti-microbial and antimutagenicity activities of pistachio (Pistachia vera) green hull extract. Food Chem. Toxicol. 2010; 48: 107–12.

13. Goli AH, Barzegar M, Sahari MA. Antioxidant activity and total phenolic compounds of pistachio (Pistachia vera) hull extracts. Food Chem. 2005; 92: 521–5.

14. Burits M, Bucar F. Antioxidant activity of Nigella sativa essential oil. Phytother. Res. 2000; 14: 323–8.

15. Musson DM, Gao R, Watson M, Lin JM, Park YE, Tuari D, et al. Bovine bone particulates containing bone anabolic factors as a potential xenogenic bone graft substitute. J. Orthop. Surg. Res. 2019; 14: 1-11.

16. Yang SB, Kim EH, Kim SH, et al. Electrospinning Fabrication of Poly (vinyl alcohol)/Coptis chinensis Extract Nanofibers for Antimicrobial Exploits. J Nanomater 2018; 8 734-748

17. Salih SI, Oleiwi JK, Ali HM, Kim YH, Oh W, Lee JT, et al. Development the Physical Properties of Polymeric Blend (SR/PMMA) by Adding Various Types of Nanoparticles, Used for Maxillofacial Prosthesis Applications. Eng. Technol. 2019; 37: 120-7.

18. Shen CL, Wang P, Guerrier J, Yeh JK, Wang JS. Protective effect of green tea polyphenols on bone loss in middle-aged female rats. Osteoporos. Int. 2008; 19: 979–90.

19. Shen CL, Yeh JK, Cao JJ, Tatum OL, Dagda RY, Wang JS. Green tea polyphenols mitigate bone loss of female rats in a chronic inflammation-induced bone loss model. J. Nutr. Biochem. 2010; 21: 968–74.

20. Seifzadeh N, Sahari MA, Barzegar M, Ahmadi Gavligh A. Concentration of pistachio hull extract antioxidants using membrane separation and reduction of membrane fouling during process. Food Sci. Nutr. 2018; 6: 1741–50.

21. Hussain L, Akash MS, Tahir M, Rehman K, Ahmed KZ. Hepatoprotective effects of methanolic extract of Alcea rosea against acetaminophen-induced hepatotoxicity in mice. Bangladesh J. Pharmacol. 2014; 9: 322-7.

22. Kandar R, Zakova P, Muzakova V. Monitoring of antioxidant properties of uric acid in humans for a consideration measuring of levels of allantoin in plasma by liquid chromatography. Clinica. Chimica. Acta. 2006; 365: 249-56.

23. Bodet C, Chandad F, Grenier D. Cranberry components inhibit interleukin-6, interleukin-8, and prostaglandin E production by lipopolysaccharide activated gingival fibroblasts. Eur. J. Oral Sci. 2007; 115: 64–70.

24. Yao Z, Xing L, Qin C. Osteoclast precursor interaction with bone matrix induces osteoclast formation directly by an interleukin-1-mediated autocrine mechanism. J. Biol. Chem. 2008; 283: 9917–24.

25. Zhao Q, Wang X, Liu Y, He A, Jia R. NFATc1: functions in osteoclasts. Int. J. Biochem. Cell. Biol. 2010; 42: 576–9.

26. Grigoriadis AE, Wang Z, Cecchini MG, Hofstetter W, Felix R, Fleischet HA, et al. c-Fos: a key regulator of osteoclast-macrophage lineage determination and bone remodeling. Science. 1994; 266: 443–8.

27. Zhang W, Liu HT, Tu LI. MAPK signal pathways in the regulation of cell proliferation in mammalian cells. Cell Res. 2002; 12: 9–18.

28. Thouverey C, Caverzasio J. The p38a MAPK positively regulates osteoblast function and postnatal bone acquisition. Cell Mol. Life Sci. 2012; 69: 3115–25.

29. Lee K, Chung YH, Ahn H, Kim H, Rho J, Jeonget D. Selective regulation of MAPK signaling mediates RANKL-dependent osteoclast differentiation. Int. J. Biol. Sci. 2016; 12: 235–45.

30. Sakai E, Shimada-Sugawara M, Yamaguchi Y, Sakamoto H, Fumimoto R, Fukuma, Y, et al. Fisetin inhibits osteoclastogenesis through prevention of RANKL-induced ROS production by Nrf2-mediated upregulation of phase II antioxidant enzymes. J. Pharmacol. Sci. 2013; 121: 288–98.

31. Heo DN, Ko WK, Moon HJ, Kim HJ, Lee SJ, Lee JB, et al. Inhibition of osteoclast differentiation by gold nanoparticles functionalized with cyclodextrin curcumin complexes. ACS Nano. 2014; 8: 12049–62.

32. Nicolin V, De Tommasi N, Nori SL, Costantinides F, Berton F, Di Lenarda R. Modulatory Effects of Plant Polyphenols on Bone Remodeling: A Prospective View from the Bench to Bedside. Front Endocrinol. 2019; 10: 494-503.

33. Oliveira I, Sousa A, Morais JS, Ferreira C, Bento A, Estevinho L, et al. Chemical composition, and antioxidant and antimicrobial activities of three hazelnuts (Corylus avellana L.) cultivars. Food Chem. Toxicol. 2008; 46: 1801–7.

34. Bouarab-Chibane L, Forquet V, Lantйri P, Clйment Y, Lйonard-Akkari L, Oulahal N, et al. Antibacterial Properties of Polyphenols: Characterization and QSAR (Quantitative Structure–Activity Relationship) Models. Front Microbiol. 2019; 10: 1-23.

35.